Highly efficient CO₂ capture with simultaneous iron and CaO recycling for the iron and steel industry†

Sicong Tian,[a] Jianguo Jiang,*[a,b,c] Feng Yan,[a] Kaimin Li,[a] Xuejing Chen[a] and Vasilije Manovic*[d]

An efficient CO₂ capture process has been developed by integrating calcium looping (CaL) and waste recycling technologies into iron and steel production. A key advantage of such a process is that CO₂ capture is accompanied by simultaneous iron and CaO recycling from waste steel slag. High-purity CaO-based CO₂ sorbents, with CaO content as high as 90 wt%, were prepared easily *via* acid extraction of steel slag using acetic acid. The steel slag-derived CO₂ sorbents exhibited better CO₂ reactivity and slower (linear) deactivation than commercial CaO during calcium looping cycles. Importantly, the recycling efficiency of iron from steel slag with an acid extraction is improved significantly due to a simultaneous increase in the recovery of iron-rich materials and the iron content of the materials recovered. High-quality iron ore with iron content of 55.1–70.6% has been recovered from waste slag in this study. Although costing nearly six times as much as naturally derived CaO in the purchase of feedstock, the final cost of the steel slag-derived, CaO-based sorbent developed is compensated by the byproducts recovered, *i.e.*, high-purity CaO, high-quality iron ore, and acetone. This could reduce the cost of the steel slag-derived CO₂ sorbent to 57.7 € t⁻¹, appreciably lower than that of the naturally derived CaO. The proposed integrated CO₂ capture process using steel slag-derived, CaO-based CO₂ sorbents developed appears to be cost-effective and promising for CO₂ abatement from the iron and steel industry.

1. Introduction

CO₂ emissions from industry are increasing, having reached 13.14 Gt in 2010 and making up 40% of the total anthropogenic CO₂ emissions worldwide.[1,2] In addition, industrial energy consumption worldwide is expected to grow from 211 EJ in 2010 to 324 EJ in 2040 due to global industrialization, mainly in Asia, Africa, South America, and the Arab countries.[3] This will result in an increase in total industrial CO₂ emissions of 74–91% by 2050 compared to 2007.[4] However, to limit the increase in the global average temperature to 2 °C, direct CO₂ emissions from industry must be 24% lower by 2050 than those in 2007.[4,5] Therefore, large energy-intensive industries manufacturing iron and steel, cement, and petrochemicals, which account for more than half of total industrial CO₂ emissions, should be the first targets to be completely decarbonized by 2050.

Implementation of CO₂ capture technologies in existing industrial sectors is urgently required, as carbon capture and storage (CCS) is the only current technology that would allow industrial sectors to realize a deep reduction in CO₂ emissions.[6] The development of CCS in various industrial sectors is springing up worldwide, leaving much room for deploying applicable technologies for industrial CO₂ capture.[7] As a promising alternative to conventional amine scrubbing and oxy-fuel combustion CO₂ capture technologies, calcium looping (CaL), which relies on CaO as a regenerable CO₂ sorbent upon cyclic carbonation and calcination reactions,[8] has been widely investigated recently through bench- and pilot-scale demonstrations at sizes of 1 kW_th–1.7 MW_th.[9–12] A recent techno-economic analysis of post-combustion CO₂ capture technologies found that CaL is more energy-efficient and cost-effective than other emerging CO₂ capture technologies, including chilled ammonia absorption, alkali–metal carbonate adsorption, and membrane separation;[13] a further reduction in the CO₂ capture cost can be achieved by integrating CaL with thermal energy storage.[14]

However, the dramatic decay in the cyclic CO₂ capture performance of naturally occurring precursors-derived CaO, trig-

[a]*School of Environment, Tsinghua University, Beijing 100084, P. R. China.*
E-mail: jianguoj@tsinghua.edu.cn
[b]*Key Laboratory for Solid Waste Management and Environment Safety, Ministry of Education of China, P. R. China*
[c]*Collaborative Innovation Center for Regional Environmental Quality, Tsinghua University, Beijing, P. R. China*
[d]*Combustion and CCS Centre, Cranfield University, Bedford, Bedfordshire, MK43 0AL, UK. E-mail: v.manovic@cranfield.ac.uk*
†Electronic supplementary information (ESI) available. See DOI: 10.1039/c6gc00400h

gered mainly by sintering of $CaCO_3$ during the CaL-based CO_2 capture process, remains as an obstacle for the development and implementation of this technology. To overcome this limitation, various strategies have been investigated to date. Several measures, including thermal activation,[15–17] steam hydration,[18–21] and recarbonation,[22] have been demonstrated to be effective in stabilizing the CO_2 capture performance of naturally occurring sorbents. Another approach involves developing synthetic CaO-based CO_2 sorbents with thermally stable surface areas and pore volumes, thereby minimizing performance deterioration for CO_2 capture. This can be achieved by employing organic-carbon templates[23–25] during sorbent preparation and introducing refractory supports[26–28] into the CaO matrix. Broda and colleagues[29] developed a highly effective MgO-stabilized, CaO-based CO_2 sorbent *via* recrystallization of calcium and magnesium acetates in organic solvents. The as-prepared material exhibited an excellent CO_2 uptake of 10.71 $mmol_{CO_2}$ $g_{sorbent}^{-1}$ after 10 harsh CaL cycles, with only 8 wt% of MgO required. However, the significantly increased cost for sorbent preparation due to the employment of organic acids should be considered before practical application.[30,31]

The iron and steel industry is the largest energy-consuming manufacturing industry in the world.[32] Currently, more than 2.5 Gt of CO_2 is emitted annually from the global iron and steel industry without implementation of any effective CO_2 reduction measures.[33] In addition to an urgent demand for CO_2 abatement in the iron and steel industry, valorization of steel slag, a Ca-rich and Fe-containing industrial waste, is another challenge faced in iron and steel production. Global annual generation of steel slag is almost 200 Mt a^{-1}, half of which is contributed by China.[34] However, only 20% of the steel slag produced annually in China is utilized, and the other 80% is stockpiled in the open air.

The CaL-based CO_2 capture process can be operated readily in a dual circulating fluidized bed system with regard to practical applications.[10] Importantly, limestone is an essential feedstock for many energy-intensive manufacturing industries (*e.g.*, the iron-and-steel and cement industries),[32,35] making it feasible for integration into industrial processes for CO_2 abatement. The potential synergy among power generation, cement production, and CO_2 abatement in the cement industry has been investigated by integrating CaL into cement manufacturing processes, where spent CaO from the CaL cycle is reused directly as a "carbon-free" feedstock for cement production, resulting in almost zero sorbent cost and waste production for CO_2 capture from the cement industry.[35–38] However, no research on the integration of CaL into the iron and steel industry for CO_2 abatement has been reported to date. Therefore, we have developed an efficient CO_2 capture process (Fig. 1) by integrating CaL and waste recycling technologies into iron and steel production to help realize simultaneous CO_2 abatement and steel slag minimization in the iron and steel industry. In this system, Ca and Fe in the steel slag are separated *via* the leaching of steel slag using acetic acid solution (acid extraction), with Ca extracted into the leachate and Fe concentrated in the residues. The Fe-rich materials can be
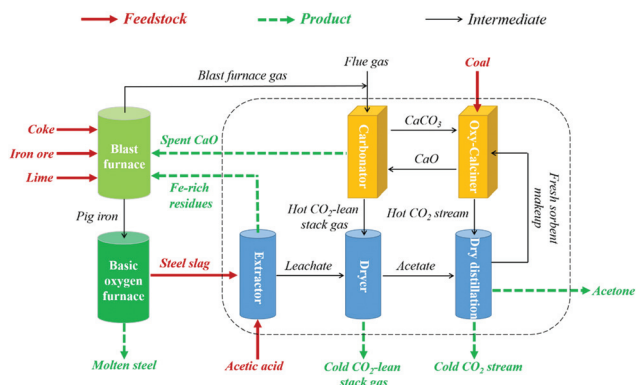

Fig. 1 General schematic of integrated CO_2 capture and steel slag valorization process proposed for use in iron and steel industry.

recycled directly into the blast furnace, substituting for iron ore as the feedstock for iron production after magnetic separation. The CaO-based sorbent, derived from the precipitation of ions in the Ca-rich leachate and a subsequent dry-distillation of the resulting precipitate, is delivered to the CaL unit for CO_2 capture. The spent sorbent can also be recycled into the blast furnace as a substitute for natural limestone to remove impurities in the iron ore during iron production. Such an integrated CO_2 capture process is demonstrated to be highly efficient and cost-effective in this study, which is promising for application to CO_2 abatement in the iron and steel industry.

2. Experimental section

2.1 Material preparation

Steel slag sample. The steel slag used in this study was obtained from the Beijing Shougang Steel Company in Qian'an, Hebei Province, China. The fresh slag, sampled after washing and crushing, was dried overnight at 105 °C and passed through a 0.1 mm sieve before use. The major elemental composition (expressed in the form of oxides) of the raw steel slag was 46.4 wt% CaO, 18.1 wt% Fe_2O_3, 14.5 wt% SiO_2, 11.6 wt% Al_2O_3, 4.7 wt% MgO, and 1.3 wt% MnO, as determined by X-ray fluorescence (XRF, XRF-1800 Analyzer, Shimadzu, Japan).

Preparation of CO_2 sorbents from steel slag. The CaO-based CO_2 sorbents were derived from steel slag using an acid extraction–precipitation approach (Scheme 1). In a typical synthesis, the steel slag sample was mixed with a 1 M solution of acetic acid at a solid/liquid ratio of 1 g to 10 mL. The mixture was stirred mechanically at room temperature for 0.5 h. Then, the steel-slag leachate was obtained by centrifugation of the slurry using a high-speed refrigerated centrifuge (himac CR22G, Hitachi, Japan), and the remaining steel-slag residues were gathered and dried for use in the iron recycling experiment described below. The obtained steel-slag leachate was directly dried overnight at 105 °C. Table 1 summarizes the parameter ranges investigated in this study. For brevity, the following
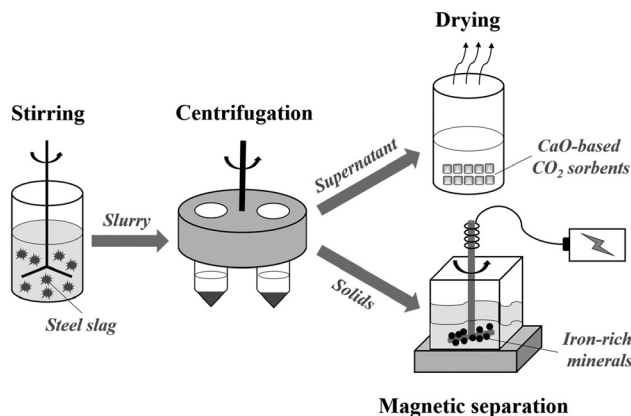
Scheme 1 Sketch of operation route for preparing CaO-based CO_2 sorbents and recovering iron-rich minerals from steel slag.

Table 1 Summary of the materials synthesized

Material	Acid concentration [M]	Extraction time [h]	Solid/liquid ratio [g : mL]
1 M–0.5 h–1 : 10	1	0.5	1 : 10
1 M–2 h–1 : 10	1	2	1 : 10
2 M–0.5 h–1 : 5	2	0.5	1 : 5
2 M–2 h–1 : 5	2	2	1 : 5
3 M–2 h–1 : 10	3	2	1 : 10
5 M–2 h–1 : 10	5	2	1 : 10

notation is used to refer to the materials synthesized: the initial concentration of acetic acid mixed with steel slag is followed by the extraction time, and the last number specifies the ratio of steel slag (g) to acetic acid solution (mL).

Recycling of iron from the remaining steel-slag residues. The experiments for recycling iron from raw steel slag and the steel-slag residues remaining after acid extraction were performed in a centrifugal-magnetic separator (CMS, KMS-181E, KEEZO, China), with a magnetic stirrer placed near the bottom of the separating chamber. The stirrer can maintain rotation at a specific centrifugal speed when the magnetic flux density on the surface of the stirrer is fixed at a desired value. Thus, phases with magnetic force from the stirrer strong enough to balance the centrifugal force it bears are separated. During the experiment, approximately 5 g of each residue or slag was placed into the chamber and the magnetic separation process was performed under a magnetic flux density of 0.4 T at different centrifugal speeds (100, 300, and 500 rpm) for 3 min.

2.2 Material characterization

Concentrations of Ca, Mg, Fe, Mn, Al, and Si in the steel slag leachate were detected using an inductively coupled plasma-atomic emission spectrometer (ICP-AES, iCAP7400, Thermo Scientific, USA). The iron content in the magnetically separated materials was determined using an X-ray Fluorescence (XRF) analyzer (Niton XL2, Thermo Scientific, USA). Powder X-ray diffraction (XRD) was performed to determine the phase

composition of the materials synthesized using an X-ray diffractometer (Smartlab, Rigaku, Japan) with the operating parameters of Cu Kα radiation (λ = 1.5418 Å) and a 40 kV/150 mA power generator. An angular range of 10–90° 2θ was measured, with a step size of 0.02° and counting time of 2 s per step. The morphology of the materials synthesized was observed using a Merlin scanning electron microscope (SEM, Zeiss, Germany), all samples were sputter-coated with an approximately 5 nm-thick layer of platinum before observation.

2.3 CO_2 sorbent test

The nitrogen temperature-programmed decomposition (N_2-TPD) experiments were performed in a thermo-gravimetric analyzer (TGA, TGA/DSC 2, Mettler Toledo). A small amount of material (~25 mg) was placed in a 150 μL alumina pan and heated to 900 °C at a rate of 10 °C min^{-1} under a N_2 flow of 50 mL min^{-1}. A mass spectrograph (MS, ThermoStar, Pfeiffer Vacuum, Germany) was connected to the TGA to simultaneously monitor the change in gas compositions in the reaction atmosphere.

The cyclic CO_2 capture experiments were performed in the TGA with a precision of 0.001 mg. During each run, a small amount (~25 mg) of sorbent was placed in a 150 μL alumina pan and heated to 900 °C at a rate of 20 °C min^{-1} under a N_2 flow of 50 mL min^{-1}. The temperature was held at 900 °C to calcine the sorbent for 10 min. Subsequently, the temperature was decreased to 650 °C at a rate of 50 °C min^{-1}. Once the reaction temperature was reached, a gas flow of 75 mL min^{-1} containing 20 vol% CO_2 and 80 vol% N_2 was introduced into the reaction chamber to carbonate the sample for 10 min. Then, the reaction atmosphere was switched to a gas flow of 75 mL min^{-1} containing 80 vol% CO_2 and 20 vol% N_2, and the sample was heated to 900 °C at a rate of 50 °C min^{-1}. After calcination at 900 °C for 5 min, a new CaL cycle was started by decreasing the reaction temperature to 650 °C under a N_2 flow of 75 mL min^{-1}. The carbonation–calcination cycle was repeated 20 times for each sorbent. The cyclic uptake of CO_2, expressed in g_{CO_2} $g_{sorbent}^{-1}$, was calculated from the continuously monitored weight change of the sample. Blank runs were performed to correct for the effects of buoyancy and change in gas density between different reaction steps.

CO_2 capture characteristics of the steel slag-derived, CaO-based CO_2 sorbents were also investigated by carbonating the material at 650 °C under a 20 vol% CO_2/80 vol% N_2 atmosphere for 120 min using TGA/DSC 2, after a pre-calcination of the sorbent at 900 °C under a N_2 atmosphere for 10 min.

3. Results and discussion

3.1 Recycling of CaO and iron from steel slag

Ca and Mg are the main elements extracted from steel slag; other major elements include Fe, Si, Mn and Al (Fig. 2). This is in line with the elemental composition of the freshly calcined CO_2 sorbents prepared from the steel slag leachate, determined by using XRF (Table S1, ESI†). It was also revealed from
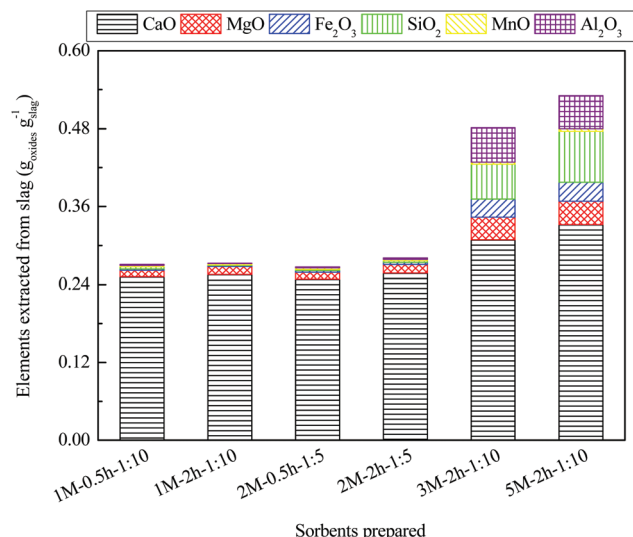
Fig. 2 Elements recovered from steel slag during acid extraction.

Fig. 3 Recycling efficiency of iron from raw steel slag and the steel slag with an acid extraction using magnetic separation with a magnetic field intensity of 0.4 T: (a) recovery of the magnetically-separated materials and (b) the iron content of the magnetically-separated materials.

Fig. 2 that the extraction time and solid/liquid ratio did not result in any significant change in the amount of elements extracted from the slag sample, yielding approximately 0.27 g of CO_2 sorbents per gram of steel slag used. This is encouraging, as a shorter extraction time and higher solid/liquid ratio are required for practical application. The amount of Ca and Mg extracted from slag increased gradually with an increasing mass ratio of acid to slag; however, this limited increase was at the cost of a higher dosage and lower conversion of acetic acid. In addition, the higher dosage (i.e., mass ratio of acid to slag) resulted in a significant increase in the amount of Fe, Si, and Al extracted, which in turn lowered the total mass fraction of CaO and MgO from 96.3% (1 M–2 h–1 : 10) to 74.0% (5 M–2 h–1 : 10) in the freshly calcined sorbents prepared. For the freshly calcined 1 M–0.5 h–1 : 10, 1 M–2 h–1 : 10, 2 M–0.5 h–1 : 5, and 2 M–2 h–1 : 5 materials with a low acid-to-slag mass ratio of 0.6 : 1, high CaO purities of ~90% could be achieved (Table S1†), indicative of a promising alternative for natural limestone as feedstock for iron production.

Fig. 3 plots the recycling efficiency of iron from the steel slag with an acid extraction, with raw steel slag included for comparison. It is shown in Fig. 3(a) that recovery of all magnetically-separated materials decreased with increasing centrifugal speed, regardless of whether raw slag or the slag with an acid extraction was employed. This is because a stronger magnetic force is required to separate phases at a higher centrifugal speed. However, there was a significant increase in the recovery of the magnetically-separated materials from the steel slag with an acid extraction compared with that from the raw slag. Increasing the dosage of acetic acid from 1 M to 3 M or 5 M during the acid extraction did not significantly increase the recovery of the magnetically-separated materials, probably because more iron was extracted into the leachate from the steel slag with higher concentrations of acetic acid as shown in Fig. 2. The iron content of the magnetically-separated
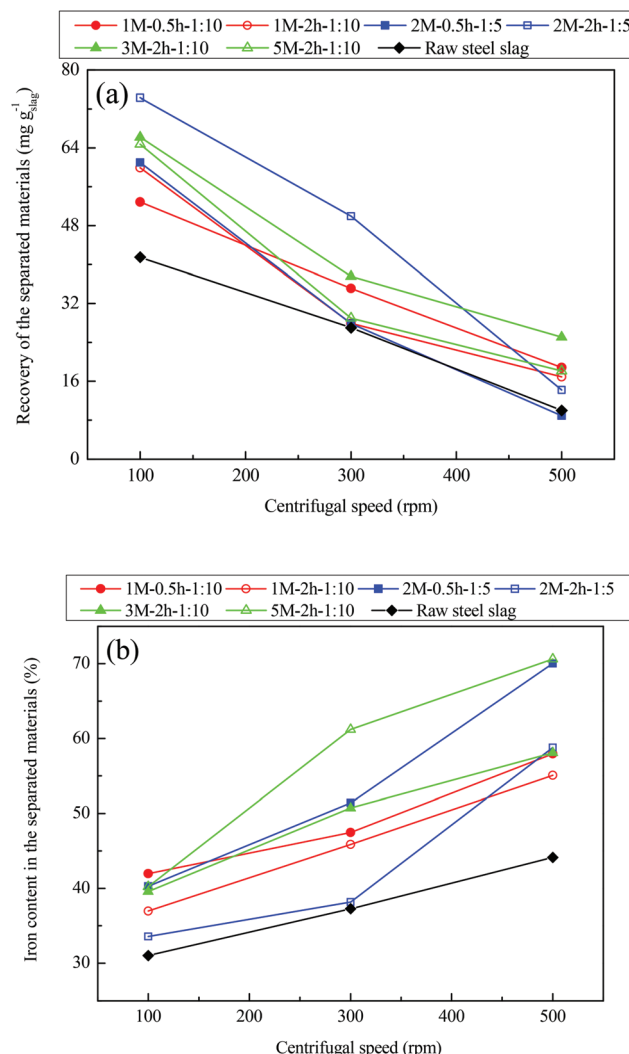
materials from either the raw steel slag or the steel slag with an acid extraction increased with centrifugal speed (Fig. 3(b)); this is because the more magnetic phases could be separated at higher centrifugal speeds. Importantly, the iron content of all magnetically-separated materials from the steel slag with an acid extraction was appreciably higher than that from the raw slag, exceeding 55% at a centrifugal speed of 500 rpm. The magnetically separated materials corresponding to 2 M–0.5 h–1 : 5 and 5 M–2 h–1 : 10 exhibited iron contents as high as 70.0% and 70.6%, respectively. These values were close to the theoretical iron content of 72.4% in pure magnetite, indicating that the as-separated materials could be a high-quality alternative to iron ore available for iron production. Therefore, when acid extraction of the waste steel slag is used, not only is high-purity CaO obtained for use in CO_2 capture (to be discussed below) and subsequent iron production, but the recycling efficiency of iron is also improved significantly by increasing
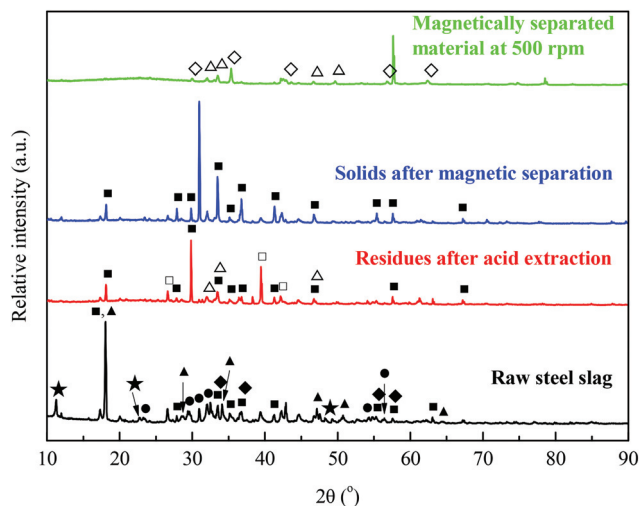
Fig. 6 SEM images of the material 1 M−2 h−1 : 10 (a) freshly dried at 105 °C, (b) heated to 600 °C, (c) heated to 900 °C, and (f) after 20 real CaL cycles; with (d) fresh and (e) cycled commercial CaO included for comparison.

Fig. 7 XRD patterns of typical steel slag-derived, CaO-based CO_2 sorbents freshly calcined at 900 °C for 10 min. The following phases were identified: (■) lime, CaO; (●) periclase, MgO; (▲) calcium sulphide, CaS; (★) wadsleyite, $(MgFe)_2SiO_4$; and (◆) srebrodolskite, $Ca_2Fe_2O_5$.

and 5 M−2 h−1 : 10 did not present a clear platform between the dehydration and acetate-decomposition steps in the normalized weight curve, and more H_2O was generated during their dehydration (Fig. S1 in the ESI†). In addition, weight loss during the $CaCO_3$-decomposition step was less normalized for 3 M−2 h−1 : 10 and 5 M−2 h−1 : 10 than for the other four materials, indicative of a lower CaO content in the material, as is in line with the results shown in Table S1.†

The change in morphology of the material 1 M−2 h−1 : 10 during N_2-TPD was further characterized using scanning electron microscopy (Fig. 6). The freshly dried 1 M−2 h−1 : 10 had a coarse structure with a comparatively compact surface (Fig. 6(a)). When heated to 600 °C, acetone was released due to the decomposition of calcium acetate, resulting in a slice-shaped morphology in the material (Fig. 6(b)). With subsequent decarbonation of $CaCO_3$ before heating to 900 °C, a well-defined, porous structure, mainly comprised of fine CaO grains, formed in the freshly calcined 1 M−2 h−1 : 10 (Fig. 6(c)). XRD patterns of typical as-prepared CO_2 sorbents in the freshly calcined state are shown in Fig. 7. The major phase, CaO, along with minor phases, MgO and CaS, were identified in 1 M−0.5 h−1 : 10, 1 M−2 h−1 : 10, 2 M−0.5 h−1 : 5, and 2 M−2 h−1 : 5, the materials with the same (low) mass ratio of acetic acid to steel slag during acid extraction (Fig. S2 in the ESI†). With increasing doses of acetic acid, small quantities of $Ca_2Fe_2O_5$ and $(MgFe)_2SiO_4$ were detected in the 3 M−2 h−1 : 10 and 5 M−2 h−1 : 10 materials synthesized.
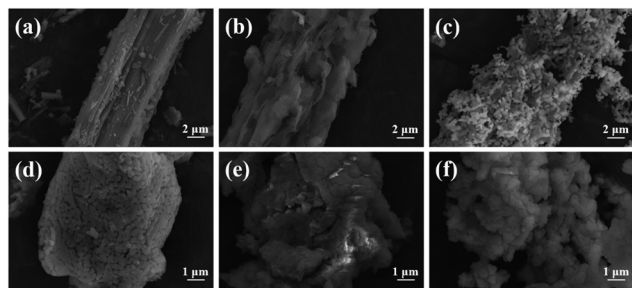
CO_2 capture performance as a function of reaction time was compared between commercial CaO and the various CaO-based CO_2 sorbents synthesized in this study (Fig. 8). Commercial CaO presented a classical two-stage CO_2 capture regime under the conditions studied here.[41] In the first 5 min, the commercial CaO experienced a fast and kinetically-controlled reaction stage as pores with a diameter <100 nm were filled by newly formed $CaCO_3$. This was followed by a substantially slower reaction stage controlled by the diffusion of CO_2 through the $CaCO_3$ product layer. Alvarez and Abanades[42] concluded that the transition between the two reaction stages occurs at a critical product layer thickness of ∼50 nm, which was better explained later by Li and colleagues[43] through a rate
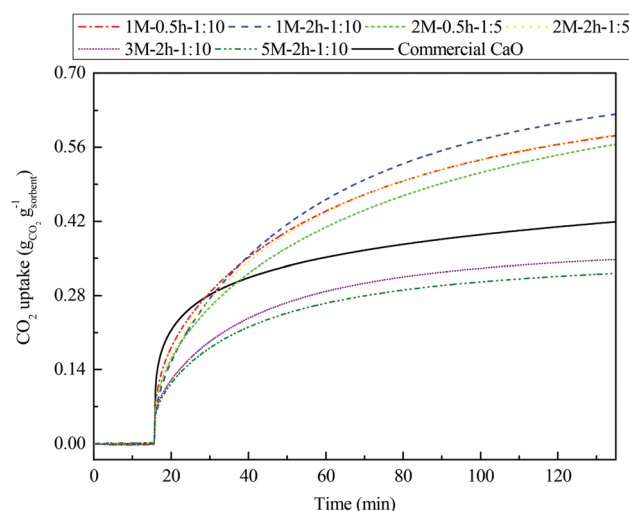
Fig. 8 Carbonation of the CO_2 sorbents synthesized, with commercial CaO included for comparison, under a 20 vol% CO_2/80 vol% N_2 atmosphere at 650 °C for 120 min.

equation theory they developed. The carbonation rate of the synthesized CaO-based CO_2 sorbents was not as fast as that of the commercial CaO during the kinetically-controlled reaction stage. However, materials 1 M−0.5 h−1 : 10, 1 M−2 h−1 : 10, 2 M−0.5 h−1 : 5, and 2 M−2 h−1 : 5 exhibited significantly faster carbonation rates than commercial CaO during the diffusion-controlled reaction stage, allowing their uptake of CO_2 to surpass that of commercial CaO after a 20 min carbonation period. After 120 min, 1 M−2 h−1 : 10 achieved a CO_2 uptake of 0.62 $g_{CO_2} g_{sorbent}^{-1}$, which was 1.5 times as high as that of the commercial CaO, indicative of an activation effect of acetic acid on the CaO-based CO_2 sorbents.[44] Freshly calcined 1 M−

0.5 h–1 : 10, 1 M–2 h–1 : 10, 2 M–0.5 h–1 : 5, and 2 M–2 h–1 : 5 exhibited similar uptakes of CO_2, indicating that the extraction time and solid/liquid ratio did not influence significantly the isothermal CO_2 capture performance of the steel slag-derived CO_2 sorbents. This is probably because the extraction time and solid/liquid ratio had almost no effect on the elemental (Table S1†) and mineral (Fig. S2†) compositions of materials. However, the CO_2 uptake experienced a significant decrease with increasing acetic acid dosage, which was likely associated with the lower CaO content in freshly calcined 3 M–2 h–1 : 10 and 5 M–2 h–1 : 10, as discussed in Fig. 2 and Table S1.†

The multicyclic CO_2 capture performance of commercial CaO and the steel slag-derived, CaO-based CO_2 sorbents synthesized in this study under realistic CaL conditions are compared in Fig. 9. The commercial CaO presented a slightly higher CO_2 uptake of 0.27 g_{CO_2} $g_{sorbent}^{-1}$ compared with the steel slag-derived sorbents 1 M–0.5 h–1 : 10, 1 M–2 h–1 : 10, 2 M–0.5 h–1 : 5, and 2 M–2 h–1 : 5 in the first cycle, whereas 3 M–2 h–1 : 10 and 5 M–2 h–1 : 10 had lower CO_2 uptakes of 0.16 g_{CO_2} $g_{sorbent}^{-1}$ and 0.14 g_{CO_2} $g_{sorbent}^{-1}$, respectively. However, the CO_2 uptake of the commercial CaO experienced a drastic decrease within the first five cycles, and began to stabilize after falling to 0.07 g_{CO_2} $g_{sorbent}^{-1}$ by the tenth cycle. For the steel slag-derived, CaO-based CO_2 sorbents synthesized, two types of multicyclic CO_2 capture characteristics were revealed. 3 M–2 h–1 : 10 and 5 M–2 h–1 : 10, although bearing a limited CO_2 capture performance compared to commercial CaO, displayed a similar CO_2 capture characteristic as the commercial CaO, i.e., the CO_2 uptake dropped drastically during the first several cycles, followed by a comparatively stable uptake afterwards. However, 1 M–0.5 h–1 : 10, 1 M–2 h–1 : 10, 2 M–0.5 h–1 : 5, and 2 M–2 h–1 : 5, the materials with the same (low) mass ratio of acetic acid to steel slag during acid extraction, exhibited a different CO_2 capture characteristic. A drastic

decay in CO_2 uptake occurred mainly between the first two cycles. Then, the CO_2 uptake experienced a slow, linear decay with increasing CaL cycles. Because of this, the CO_2 uptake of 1 M–0.5 h–1 : 10, 1 M–2 h–1 : 10, 2 M–0.5 h–1 : 5, and 2 M–2 h–1 : 5 exceeded that of the commercial CaO from the third cycle onward, and 1 M–2 h–1 : 10 captured almost twice as much CO_2 as the commercial CaO by the end of the twentieth cycle. One would expect that the well-preserved porous structure of the cycled 1 M–2 h–1 : 10, compared to that of the commercial CaO, ensured its favorable CO_2 capture characteristics (Fig. 6(c–f)). Therefore, the better carbonation reactivity (Fig. 8) and cyclic stability (Fig. 9) of the steel slag-derived, CaO-based CO_2 sorbents 1 M–0.5 h–1 : 10, 1 M–2h–1 : 10, 2 M–0.5 h–1 : 5, and 2 M–2 h–1 : 5, when compared to commercial CaO, suggest that they are promising alternatives for use in CaL.

3.3 Preliminary cost structure of the proposed integrated CO_2 capture process

One inherent advantage of CaL over any other current post-combustion CO_2 capture technologies, when employed for CO_2 abatement in the iron and steel industry, is that the spent CaO can be recycled directly as a flux into the blast furnace for iron production. This would result in an additional reduction in CO_2 emissions associated with the calcination of limestone during conventional iron and steel production processes. With regard to the practical application of CaL-based CO_2 capture technology, the cost structure can be affected by a variety of operating parameters. MacKenzie and colleagues[45] performed a sensitivity analysis on eight potentially key variables influencing the cost of CaL-based CO_2 capture technology used in practical applications. They confirmed that the CO_2 capture cost of the CaL process is most affected by the cost of CaO-based sorbents and their deactivation rate when the internal solid circulation (molar ratio of CaO to CO_2) and the make-up flow of solids (purge percentage of fresh CaO in the calciner) have been determined. The superior CO_2 reactivity and favorable deactivation rate of the steel slag-derived, CaO-based materials 1 M–0.5 h–1 : 10, 1 M–2 h–1 : 10, 2 M–0.5 h–1 : 5, and 2 M–2 h–1 : 5, when compared to the commercial CaO, have been verified above. Now we attempt to compare the preliminary cost structure between limestone-derived CaO and typical steel slag-derived CO_2 sorbents developed in this study, mainly based on the material flow analysis, as shown in Table 2. Naturally occurring limestone is the main feedstock of conventional CaO-based CO_2 sorbent for CaL. For the steel slag-derived, CaO-based CO_2 sorbents developed in this study, given that steel slag is an almost zero-cost industrial waste, acetic acid is the main consideration in the cost analysis. For materials 1 M–0.5 h–1 : 10 and 1 M–2 h–1 : 10, ~2.5 g of acetic acid was consumed to produce 1 g of CO_2 sorbent, which is near the theoretically lowest requirement of ~2.1 $g_{acetic\ acid}$ $g_{sorbent}^{-1}$. Although bearing a higher expense for feedstock than naturally derived CaO, the final cost of the steel slag-derived, CaO-based sorbent was well compensated by the byproducts recovered, i.e., the high-purity CaO, high-quality iron ore, and acetone. The cost of materials 1 M–0.5 h–1 : 10 and 1 M–2 h–1 : 10 was
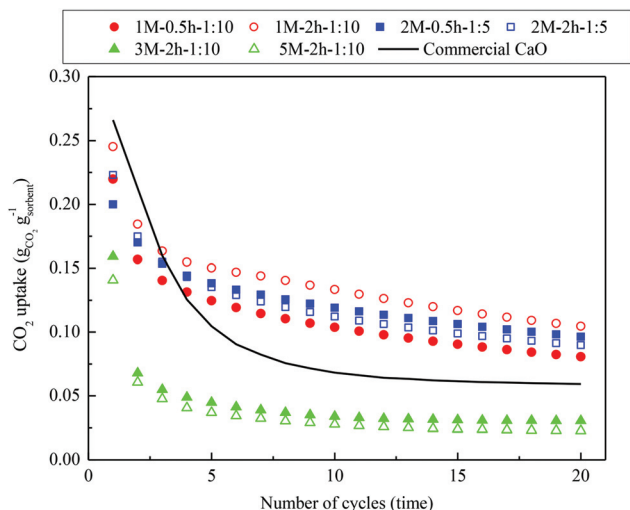

Fig. 9 Multicyclic CO_2 capture performance of the steel slag-derived, CaO-based sorbents synthesized, with commercial CaO included for comparison, under realistic CaL conditions.

Table 2 Comparison of sorbent costs based on material flow analysis

Material	Feedstock consumed[a] [t $t_{sorbent}^{-1}$]		Byproduct recovered[a] [t $t_{sorbent}^{-1}$]			Cost of sorbents [€ t^{-1}]
	Acetic acid	Limestone	CaO	Iron ore	Acetone	
1 M–0.5 h–1 : 10	2.50	—	0.91	0.05	0.94	57.7
1 M–2 h–1 : 10	2.50	—	0.90	0.06	0.93	62.2
2 M–0.5 h–1 : 5	2.86	—	0.90	0.06	0.93	145.7
2 M–2 h–1 : 5	2.73	—	0.89	0.07	0.92	120.0
Naturally derived CaO	—[b]	1.98	—	—	—	102.0

[a] Prices of the components mentioned were determined according to the average price from the past 3 years in the Chinese market, *i.e.*, 231.9 € t^{-1}, 51.5 € t^{-1}, 103.1 € t^{-1}, and 450.9 € t^{-1} for acetic acid (≥99.8 wt%), limestone (~90 wt%), iron ore (~62 wt%), and acetone (≥99.5 wt%), respectively. [b] The component was not consumed or recovered.

Table 3 Maximum acceptable cost of the steel slag-derived, CaO-based CO_2 sorbents developed under various CaL conditions

Material	X_{ave} increase[a] [%]	Maximum acceptable cost of sorbents [€ t^{-1}]					
		R[b] = 1.5		R = 3		R = 5	
		f_p[c] = 1%	f_p = 2.5%	f_p = 1%	f_p = 2.5%	f_p = 1%	f_p = 2.5%
1 M–0.5 h–1 : 10	3.8	117.2	109.4	112.6	109.7	111.4	108.9
1 M–2 h–1 : 10	7.6	132.3	116.7	123.3	117.3	120.8	115.9
2 M–0.5 h–1 : 5	5.9	125.6	113.4	118.5	113.9	116.6	112.8
2 M–2 h–1 : 5	5.4	123.6	112.5	117.1	112.9	115.4	111.8

[a] The subtraction of average carbonation conversion during 20 cycles between the steel slag-derived CO_2 sorbent and naturally derived CaO. [b] The molar ratio of the CaO-based sorbent to CO_2 during the CaL process. [c] The make-up flow (purge percentage) of fresh CaO-based sorbents in the calciner.

57.7 € t^{-1} and 62.2 € t^{-1}, respectively, appreciably lower than that of the naturally derived CaO (102 € t^{-1}).

Given the enhanced CO_2 capture performance of the steel slag-derived sorbents compared to naturally derived CaO, an increase in the cost of the as-prepared CO_2 sorbents is acceptable as long as it remains below an upper limit, which largely depends on the CO_2 capture capacity of the materials. Romeo and colleagues[46] studied in detail the relationship between the increase in the maximum average CO_2 capture capacity of CaO-based sorbents and the maximum acceptable investment in sorbents under different CaL operations, and proposed a useful approach to assess the availability of new CaO-based CO_2 sorbents for use in CaL; we adapted this approach to assess the acceptable cost of the steel slag-derived CO_2 sorbents developed in this study (Table 3). As expected, a more cost-effective CaO-based CO_2 sorbent is required when CaL is performed under higher sorbent-to-CO_2 ratios (R) or material make-up flows (f_p), as more fresh sorbents are consumed under these operating conditions. Materials 1 M–0.5 h–1 : 10 and 1 M–2 h–1 : 10 exhibited appreciable superiority over naturally derived CaO with regard to the cost of sorbents under all sorbent/CO_2 ratios and material make-up flows. Material 2 M–2 h–1 : 5 was comparable with naturally derived CaO under low sorbent/CO_2 ratios and material make-up flows, while the cost of material 2 M–0.5 h–1 : 5 was marginally higher than naturally derived CaO. However, it should be pointed out that the cost structure of the proposed integrated CO_2 capture process was assessed here mainly based on the material flow analysis. The capital costs and variable operating costs commonly considered in practical CaL projects have not been mentioned yet at this stage. Nevertheless, the proposed integrated CO_2 capture process using materials 1 M–0.5 h–1 : 10 and 1 M–2 h–1 : 10 appears to be cost-effective, which is promising for CO_2 abatement applications in the iron and steel industry.

4. Conclusions

We have proposed and experimentally demonstrated the feasibility of an integrated CO_2 capture process for CO_2 abatement in the iron and steel industry. In such a process, highly effective CaO-based CO_2 sorbents were easily prepared *via* acid extraction of waste steel slag using acetic acid. Encouragingly, the recycling efficiency of iron from the steel slag residues remaining after acid extraction increased significantly due to improvement in both the recovery of iron-rich materials and the iron content in the materials recovered, allowing for recycling of high-quality iron ore with iron content as high as 55.1–70.6%. The steel slag-derived, CaO-based CO_2 sorbents 1 M–0.5 h–1 : 10, 1 M–2 h–1 : 10, 2 M–0.5 h–1 : 5, and 2 M–2 h–1 : 5 could achieve CaO content as high as ~90 wt%. The well-defined, porous morphology ensured these materials superior CO_2 reactivity, and importantly, significantly slower linear deactivation with CaL cycles, compared to commercial

CaO. Although costing more than naturally derived CaO in the purchase of feedstock, the final cost of the steel slag-derived, CaO-based CO_2 sorbent developed here was compensated by the byproducts recovered, *i.e.*, the high-purity CaO, high-quality iron ore, and acetone. Materials 1 M–0.5 h–1 : 10 and 1 M–2 h–1 : 10 were much more cost-effective than naturally derived CaO, making the integrated CO_2 capture process proposed in this study potentially very attractive for CO_2 abatement in the iron and steel industry.

Acknowledgements

References

1 IPCC, Industry, in *Climate Change 2014: Mitigation of Climate Change. Contribution of Working Group III to the Fifth Assessment Report of the Intergovernmental Panel on Climate Change*, Cambridge University Press, Cambridge, United Kingdom and New York, NY, USA, 2014.

2 T. A. Napp, A. Gambhir, T. P. Hills, N. Florin and P. S. Fennell, A review of the technologies, economics and policy instruments for decarbonising energy-intensive manufacturing industries, *Renewable Sustainable Energy Rev.*, 2014, **30**, 616–640.

3 U.S. Energy Information Administration (U.S. EIA), International Energy Outlook 2013: With Projections to 2040, Washington, DC 20585; 2013. To be found at: http://www.eia.gov/forecasts/ieo/pdf/0484(2013).pdf.

4 International Energy Agency (IEA), *Energy technology perspectives 2010: scenarios & strategies to 2050*, OECD/IEA, Paris and 2010.

5 IPCC, Climate Change 2007: Synthesis Report. Contribution of Working Groups I, II and III to the Fourth Assessment Report of the Intergovernmental Panel on Climate Change, Geneva, Switzerland, 2007.

6 International Energy Agency (IEA), *Executive Summary for Energy Technology Perspectives 2012: Pathways to a Clean Energy System*, OECD/IEA, Paris, 2012. To be found at: http://www.iea.org/textbase/npsum/ETP2012SUM.pdf.

7 International Energy Agency (IEA), *Tracking Clean Energy Progress 2014*, OECD/IEA, Paris, 2014. To be found at: http://www.iea.org/publications/freepublications/publication/Tracking_clean_energy_progress_2014.pdf.

8 S. Tian, J. Jiang, F. Yan, K. Li and X. Chen, Synthesis of highly efficient CaO-based, self-stabilizing CO_2 sorbents via structure-reforming of steel slag, *Environ. Sci. Technol.*, 2015, **49**, 7464–7472.

9 D. P. Hanak, E. J. Anthony and V. Manovic, A review of developments in pilot-plant testing and modelling of calcium looping process for CO_2 capture from power generation systems, *Energy Environ. Sci.*, 2015, **8**, 2199–2249.

10 B. Arias, M. E. Diego, J. C. Abanades, M. Lorenzo, L. Diaz, D. Martínez, J. Alvarez and A. Sánchez-Biezma, Demonstration of steady state CO_2 capture in a 1.7 MW$_{th}$ calcium looping pilot, *Int. J. Greenhouse Gas Control*, 2013, **18**, 237–245.

11 J. Blamey, E. J. Anthony, J. Wang and P. S. Fennell, The calcium looping cycle for large-scale CO_2 capture, *Prog. Energy Combust. Sci.*, 2010, **36**, 260–279.

12 M. Alonso, M. E. Diego, C. Perez, J. R. Chamberlain and J. C. Abanades, Biomass combustion with in situ CO_2 capture by CaO in a 300 kWth circulating fluidized bed facility, *Int. J. Greenhouse Gas Control*, 2014, **29**, 142–152.

13 M. Zhao, A. I. Minett and A. T. Harris, A review of techno-economic models for the retrofitting of conventional pulverised-coal power plants for post-combustion capture (PCC) of CO_2, *Energy Environ. Sci.*, 2013, **6**, 25–40.

14 D. P. Hanak, C. Biliyok and V. Manovic, Calcium looping with inherent energy storage for decarbonisation of coal-fired power plant, *Energy Environ. Sci.*, 2016, **9**, 971–983.

15 D. C. Ozcan, B. H. Shanks and T. D. Wheelock, Improving the stability of a CaO-based sorbent for CO_2 by thermal pretreatment, *Ind. Eng. Chem. Res.*, 2011, **50**, 6933–6942.

16 V. Manovic and E. J. Anthony, Thermal activation of CaO-based sorbent and self-reactivation during CO_2 capture looping cycles, *Environ. Sci. Technol.*, 2008, **42**, 4170–4174.

17 Z. Chen, H. S. Song, M. Portillo, C. J. Lim, J. R. Grace and E. J. Anthony, Long-term calcination/carbonation and thermal pretreatment for CO_2 capture by limestone and dolomite, *Energy Fuels*, 2009, **23**, 1437–1444.

18 V. Manovic and E. J. Anthony, Steam reactivation of spent CaO-based sorbent for multiple capture cycles, *Environ. Sci. Technol.*, 2007, **41**, 1420–1425.

19 B. V. Materić, C. Sheppard and S. I. Smedley, Effect of repeated steam hydration reactivation on CaO-based sorbents for CO_2 capture, *Environ. Sci. Technol.*, 2010, **44**, 9496–9501.

20 F. Donat, N. H. Florin, E. J. Anthony and P. S. Fennell, Influence of high-temperature steam on the reactivity of CaO sorbent for CO_2 capture, *Environ. Sci. Technol.*, 2012, **46**, 1262–1269.

21 N. Phalak, N. Deshpande and L. S. Fan, Investigation of high-temperature steam hydration of naturally derived calcium oxide for improved carbon dioxide capture capacity over multiple cycles, *Energy Fuels*, 2012, **26**, 3903–3909.

22 B. Arias, G. S. Grasa, M. Alonso and J. C. Abanades, Post-combustion calcium looping process with a highly stable sorbent activity by recarbonation, *Energy Environ. Sci.*, 2012, **5**, 7353–7359.

23 W. Q. Liu, B. Feng, Y. Q. Wu, G. X. Wang, J. Barry and J. C. D. da Costa, Synthesis of sintering-resistant sorbents for CO_2 capture, *Environ. Sci. Technol.*, 2010, **44**, 3093–3097.

24 M. Broda and C. R. Müller, Synthesis of highly efficient, Ca-based, Al_2O_3-stabilized, carbon gel-templated CO_2 sorbents, *Adv. Mater.*, 2012, **24**, 3059–3064.

25 S. Wang, L. Fan, C. Li, Y. Zhao and X. Ma, Porous spherical CaO-based sorbents via PSS-assisted fast precipitation for CO_2 capture, *ACS Appl. Mater. Interfaces*, 2014, **6**, 18072–18077.

26 R. Filitz, A. M. Kierzkowska, M. Broda and C. R. Müller, Highly efficient CO_2 sorbents: development of synthetic, calcium-rich dolomites, *Environ. Sci. Technol.*, 2012, **46**, 559–565.

27 F. N. Ridha, V. Manovic, A. Macchi and E. J. Anthony, High-temperature CO_2 capture cycles for CaO-based pellets with kaolin-based binders, *Int. J. Greenhouse Gas Control*, 2012, **6**, 164–170.

28 M. Zhao, J. Shi, X. Zhong, S. Tian, J. Blamey, J. Jiang and P. S. Fennell, A novel calcium looping absorbent incorporated with polymorphic spacers for hydrogen production and CO_2 capture, *Energy Environ. Sci.*, 2014, **7**, 3291–3295.

29 M. Broda, A. M. Kierzkowska and C. R. Müller, Development of highly effective CaO-based, MgO-stabilized CO_2 sorbents via a scalable "one-pot" recrystallization technique, *Adv. Funct. Mater.*, 2014, **24**, 5753–5761.

30 F. N. Ridha, V. Manovic, Y. Wu, A. Macchi and E. J. Anthony, Pelletized CaO-based sorbents treated with organic acids for enhanced CO_2 capture in Ca-looping cycles, *Int. J. Greenhouse Gas Control*, 2013, **17**, 357–365.

31 F. N. Ridha, V. Manovic, A. Macchi, M. A. Anthony and E. J. Anthony, Assessment of limestone treatment with organic acids for CO_2 capture in Ca-looping cycles, *Fuel Process. Technol.*, 2013, **116**, 284–291.

32 M. T. Ho, A. Bustamante and D. E. Wiley, Comparison of CO_2 capture economics for iron and steel mills, *Int. J. Greenhouse Gas Control*, 2013, **19**, 145–159.

33 J. Oda, K. Akimoto, T. Tomoda, M. Nagashima, K. Wada and F. Sano, International comparisons of energy efficiency in power, steel, and cement industries, *Energy Policy*, 2012, **44**, 118–129.

34 P. Renforth, C. L. Washbourne, J. Taylder and D. A. C. Manning, Silicate production and availability for mineral carbonation, *Environ. Sci. Technol.*, 2011, **45**, 2035–2041.

35 A. Telesca, D. Calabrese, M. Marroccoli, M. Tomasulo, G. L. Valenti, G. Duelli and F. Montagnaro, Spent limestone sorbent from calcium looping cycle as a raw material for the cement industry, *Fuel*, 2014, **118**, 202–205.

36 C. C. Dean, D. Dugwell and P. S. Fennell, Investigation into potential synergy between power generation, cement manufacture and CO_2 abatement using the calcium looping cycle, *Energy Environ. Sci.*, 2011, **4**, 2050–2053.

37 N. Rodríguez, R. Murillo and J. C. Abanades, CO_2 capture from cement plants using oxyfired precalcination and/or calcium looping, *Environ. Sci. Technol.*, 2012, **46**, 2460–2466.

38 K. Atsonios, P. Grammelis, S. K. Antiohos, N. Nikolopoulos and E. Kakaras, Integration of calcium looping technology in existing cement plant for CO_2 capture: process modeling and technical considerations, *Fuel*, 2015, **153**, 210–223.

39 Y. Li, C. Zhao, L. Duan, C. Liang, Q. Li, W. Zhou and H. Chen, Cyclic calcination/carbonation looping of dolomite modified with acetic acid for CO_2 capture, *Fuel Process. Technol.*, 2008, **89**, 1461–1469.

40 Y. Li, C. Zhao, H. Chen, C. Liang, L. Duan and W. Zhou, Modified CaO-based sorbent looping cycle for CO_2 mitigation, *Fuel*, 2009, **88**, 697–704.

41 J. C. Abanades, E. J. Anthony, D. Y. Lu, C. Salvador and D. Alvarez, Capture of CO_2 from combustion gases in a fluidized bed of CaO, *AIChE J.*, 2004, **50**, 1614–1622.

42 D. Alvarez and J. C. Abanades, Determination of the critical product layer thickness in the reaction of CaO with CO_2, *Ind. Eng. Chem. Res.*, 2005, **44**, 5608–5615.

43 Z. Li, H. Sun and N. Cai, Rate equation theory for the carbonation reaction of CaO with CO_2, *Energy Fuels*, 2012, **26**, 4607–4616.

44 E. R. Sacia, S. Ramkumar, N. Phalak and L. S. Fan, Synthesis and regeneration of sustainable CaO sorbents from chicken eggshells for enhanced carbon dioxide capture, *ACS Sustainable Chem. Eng.*, 2013, **1**, 903–909.

45 A. MacKenzie, D. L. Granatstein, E. J. Anthony and J. C. Abanades, Economics of CO_2 capture using the calcium cycle with a pressurized fluidized bed combustor, *Energy Fuels*, 2007, **21**, 920–926.

46 L. M. Romeo, Y. Lara, P. Lisbona and A. Martínez, Economical assessment of competitive enhanced limestones for CO_2 capture cycles in power plants, *Fuel Process. Technol.*, 2009, **90**, 803–811.